Cheng(2010) took the dome with rise-ratio of 1/2 as model, carried out the wind tunnel tests with the Reynolds of $5.3\times10^4<Re<2.0\times10^6$ in smooth flow and $5.3\times10^4<Re<1.65\times10^6$ in turbulent flow, and concluded that the transition of separation flow occurs in the Re range of 1.8×10^5 to 3.0×10^5 in smooth flow and ranged from 1.0×10^5 to 2.0×10^5 in boundary layer flow, the wind pressure distribution and wind load forces would be stable after the transitional Reynolds number.

The objective of the present study is to investigate the Reynolds number dependence of the aerodynamic loads and related properties for a dome roof with rise ratio(H/D) of 0.25 in uniform smooth and boundary turbulent flows. For this, a series of wind tunnel tests for simultaneous multi-pressure measurements of dome roofs with diameters D = 0.2, 0.6 and 1.33m were conducted. Three types of boundary turbulent flows were generated with exponential coefficient of 0.15. In particular, we focus on the effects of free-stream turbulence and Reynolds number on the wind pressure and forces, in order to determine a wind load pattern which is Reynolds number independent to be used as the reference of future experimental research. Further, investigations have also been made to clarify the effects of different flow conditions on the power spectra of fluctuating wind forces at different Reynolds numbers.

2. EXPERIMENTAL ARRANGEMENTS

The experimental investigation was carried out in a closed-circuit-type wind tunnel with a working section 25 m long, 4 m wide and 3 m high, in Harbin Institute of Technology, China. The wind tunnel tests were conducted first in smooth uniform flow condition, then in the boundary layer turbulences simulated according to Chinese Code. The schematics of wind tunnel experimental setup in Fig. 1 in smooth flow. The diameters D of dome roofs were 0.2, 0.6 and 1.33 m, namely small, medium and large models, which had the same rise to diameter ratio h/D = 0.25. The roof models were supported by a base plate elevated 0.5 m from the floor, which was used to minimize the effect of the boundary layer developed on the wind tunnel floor. (see Fig. 2). It can be observed from this figure that, in all cases, the thickness of the flat-plate turbulent boundary layer was about 60 mm. Thus, a wall height h (= 60 mm) of the cylindrical model was determined to ensure approximately uniform flows around the roofs with different turbulence intensities. The base plate had a thickness of 0.02 m, with a width of 2.4 m and a length of 4.8 m, which was long enough to ensure that the separated shear layer reattaches to the plate surface. Additionally, the plate has a sharp edge with a cutting angle of about 30º to prevent the sudden separation of the approaching flow at the leading edge. Statistics of the wind velocity fluctuation were measured by the hot-wire anemometers at the center position of the model.

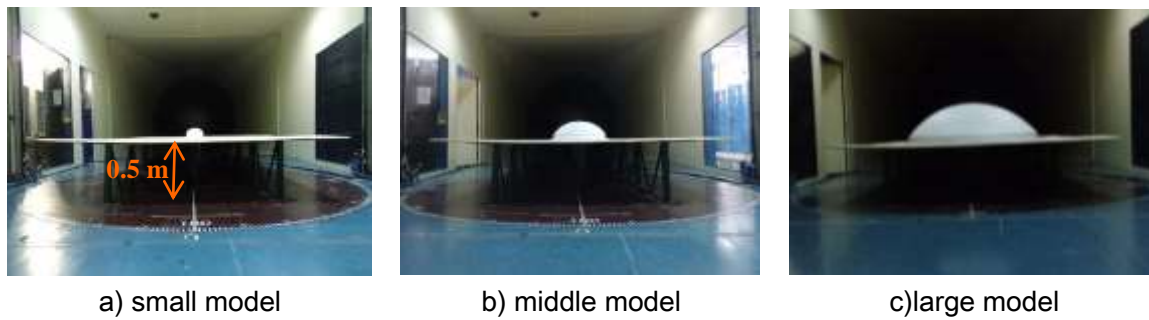| a) small model | b) middle model | c)large model |

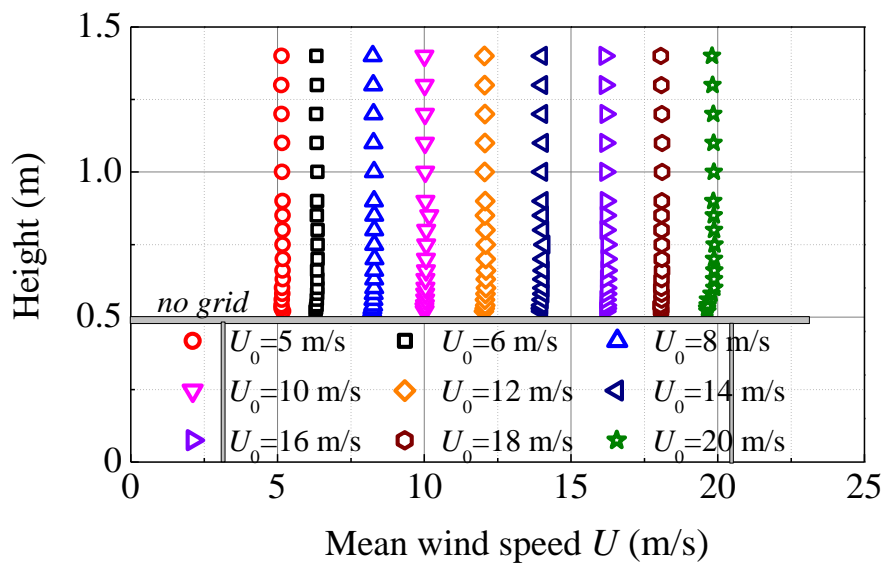Fig. 1 Pictures of wind tunnel tests in smooth flow

Fig. 2 Variations in the flat-plate turbulent boundary layer

Pressure taps were distributed uniformly over the roof surfaces with total number of 217. Instantaneous wind pressures acting on the dome roof were measured using a DSM3400 pressure scanner system. A sampling frequency of 625 Hz was employed and the measurement duration was 100 s. Each pressure tap was connected to pressure transducers via 1.0 m length polyethylene pipes with an inside diameter of 0.9 mm. The effect of the tube system, such as Helmholtz resonance on the measured pressure fluctuations, was eliminated by compensating the gain and phase shift using the transfer function obtained beforehand (Irwin et al. 1979). The maximum blockage ratio of cylindrical roof models was about 3.7% with no correction to the measured data.

3. Experimental results and discussion

The wind pressures used in this article are non-dimensionalized with respect to the kinetic pressure $0.5\rho_a U^2$, and the pressure coefficients are ensemble averages of 5 samples. Due to three model-scales were used to extend the Reynolds number range, the scaling and blockage problems may be brought out. Thus, at the very beginning of the investigation, the consistency and continuity of pressure distributions on different

roof models at overlapping Reynolds numbers were examined. Fig. 3 shows the mean pressure distributions Cp derived from these three models in smooth flow at selected Reynolds number of 2.48×10^5 and 9.12×10^5. It can be observed that the pressure distributions match well with each other. Note that, the small discrepancy between the pressure distributions may be associated with the effects of different wall height to cylinder diameter ratios.
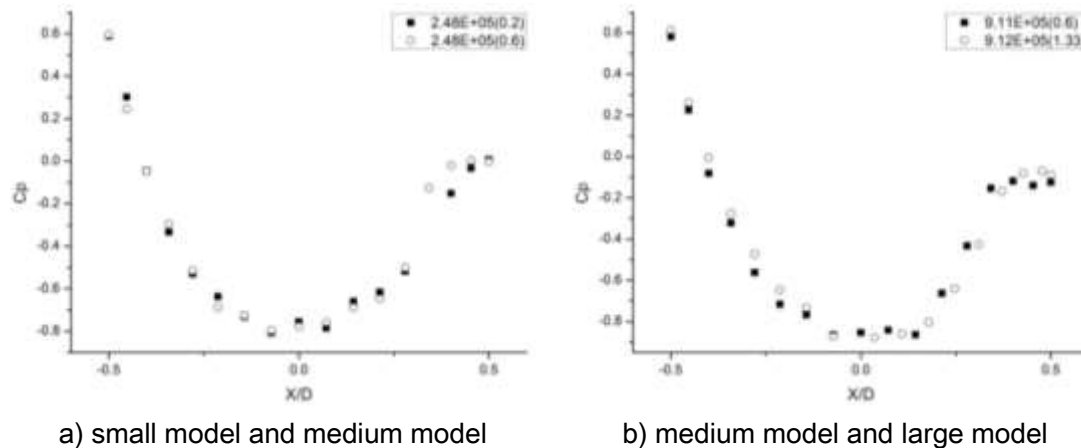
| a) small model and medium model | b) medium model and large model |

Fig. 3 Comparison of the mean pressure distributions on centerlines of small, medium and large cylindrical roofs in smooth flow.

The effects of Reynolds number on the overall pattern of pressure distributions in smooth flow are first given. Fig. 4 shows the contours of mean pressure coefficients for the dome roofs in a Reynolds number range 8.28×10^4 to 9.11×10^5. Results of the mean pressure contours show that the flow pattern exhibits a strong dependence on the Reynolds number. The peak suction over the central part of the dome roof gradually increases with Re up to 2.48×10^5, and then decreases somewhat thereafter. It is interesting to observe that, the mean pressure contour lines exhibit a roughly two-dimensional pattern perpendicular to the wind direction, except in the edge regions where a three-dimensional effect may be significant. Thus, this may suggest that the overall pattern of mean pressure distribution can be approximately evaluated by the Cp distributions along the centerline of the dome roof along wind direction.

In order to give a quantitative description of the Reynolds number effect on the pressure distribution patterns, the mean pressure coefficients along the centerline in a Re range 5.52×10^4 to 2.02×10^6 are plotted in Fig. 5. It should be noted that these two figures present the measured data from the small, medium and large models respectively, since an aerodynamic similarity between the two test models has been proved to be valid at the overlapping Reynolds numbers (as seen from Fig. 4). A clear Reynolds number trend can be observed from the mean pressure distributions, with the peak suctions (minimum Cp varies from -0.4 to -0.9) steadily increasing up to Re = 2.48×10^5 and then slightly decreasing thereafter. The wake suction gradually decreases (Cp=-0.4~ -0.1) and then increases, which is different from cylindrical roof may related to the 3-dimensional effect of dome roof. Nevertheless, the Cp in the windward region is nearly Re independent in the radial angle range between 0⁰ and 36⁰.

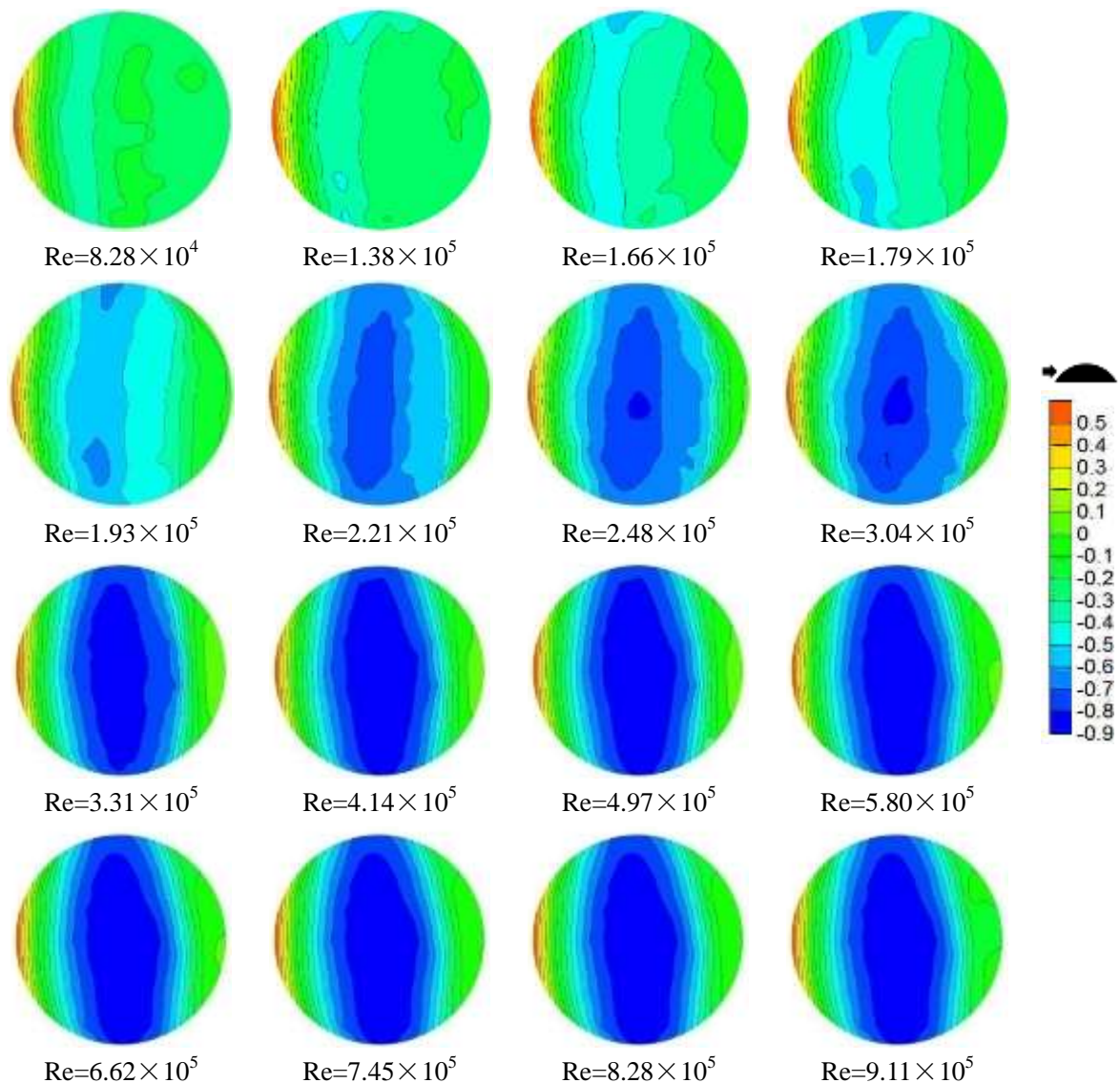Fig. 4 Contours of mean pressure coefficients for the dome roofs in a Reynolds number range 8.28×10⁴ to 9.11×10⁵

These trends discussed above may be more clearly illustrated by integrating the mean pressure distributions on the whole surface of the model, to give a drag coefficient C_d and lift coefficient C_l, as shown in Fig. 6. Here, C_d and C_l represent the dimensionless wind force in the streamwise direction (x-axis) and vertical direction (z-axis). Take the smooth flow for instance the C_d continuously decreases, whilst the C_l rapidly increases as the Reynolds number increases, up to about 2.48×10⁵. With the Reynolds number further increasing from 2.48×10⁵ to 2.02×10⁶, the C_d and C_l slightly vary with Re and gradually exhibit relatively stable values. Thus, it has suggested the possibility that the transition to turbulence in the separated shear layer occurs in a range of Re =1.66×10⁵ ~ 2.48×10⁵.

a) small model   b) medium model
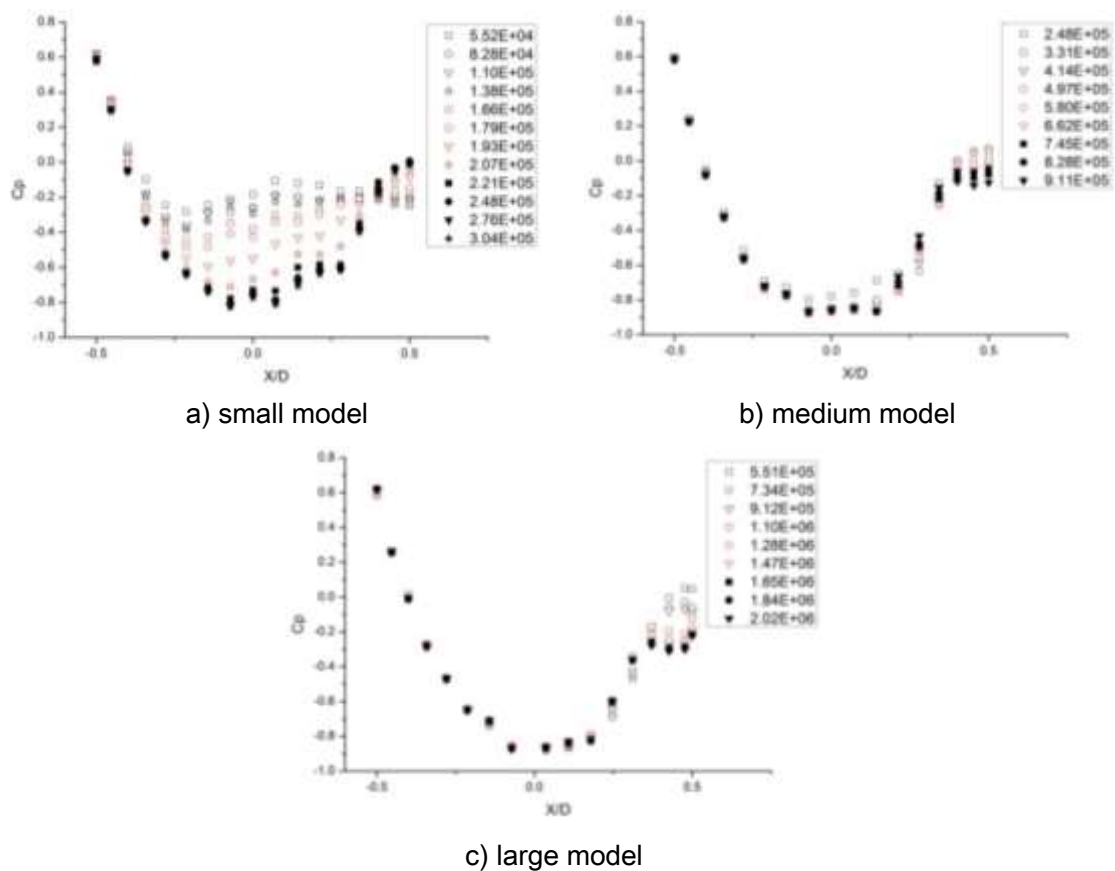

c) large model

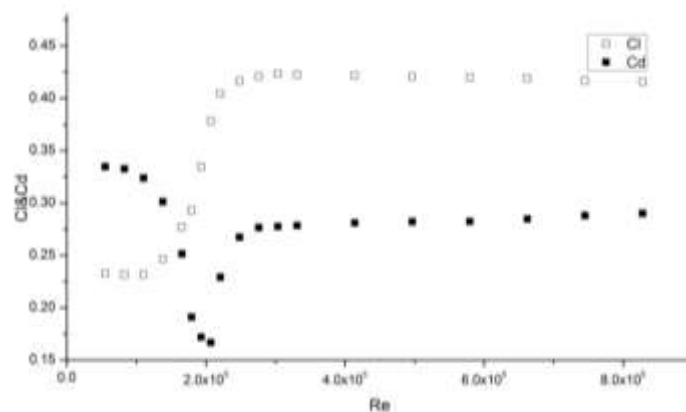Fig. 5 Representative distributions of the mean pressure coefficient on the centerline

Fig. 6 Wind force coefficients as a function of Reynolds number in smooth flow: drag coefficient C_d and lift coefficient C_l.

The distributions of the rms pressure coefficients on the centerline of the dome roof at various Reynolds numbers are shown in Fig. 7. It can be clearly observed that the Reynolds number has a relatively significant influence on the fluctuating pressure distributions in the negative pressure region, especially in the downstream region near

the separation point. In the range of Re = 8.28×10^4 ~ 1.79×10^5, Cp' gradually increases with Re and reaches its local maximum at Re = 1.66×10^5. In addition, there exists a dual-peak phenomena on the Cp' distribution in this Re range, and the first peak gradually diminishes with Re further increasing up to about 2.07×10^5. This is in agreement with Cheng and Fu's (2010) studies on a semi-spherical dome. They suggested that the dual peaks of Cp' distribution indicated the transition of the separated shear layer to turbulence happened, and a small separation bubble before the final separation was formed in this stage. While, the first and second peaks might be related with the locations of fore- and reattachment-separation bubbles. When Re > 2.20×10^5, Cp' monotonously decreases with the increasing Re, and remains nearly invariant after Re = 2.48×10^5. Therefore, based on these observations, it may be stated that the transition from laminar to turbulent flow occurs in the Re range 1.66×10^5 to 2.48×10^5, and both mean and rms pressure distributions become Reynolds number independent when Re = 2.48×10^5 ~ 2.02×10^6.
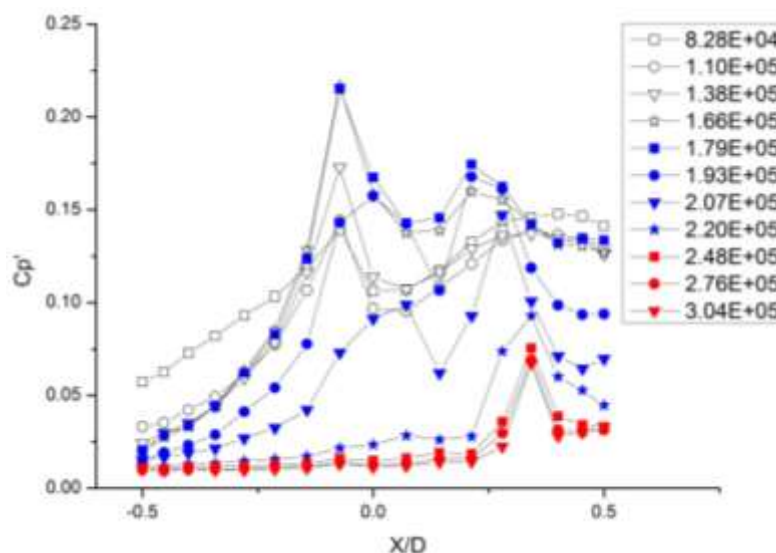

Fig. 7 Fluctuating pressure distributions on the centerlines of
the dome roofs in smooth flow

The power spectra of the fluctuating lift and drag forces in smooth flow are shown in Fig. 8 and Fig.9, in a Reynolds number range 8.28×10^4 to 9.11×10^5. Note, the fluctuating forces were calculated from the instantaneous pressures over the whole surface of the cylindrical roof. It can be observed from Fig. 8that, the spectral peaks of the lift force occur at relatively low reduced frequencies from about 0.01 to 0.1. And as the Reynolds number increases, the bandwidth of the spectra is gradually narrowed. However, for the drag force spectra see Fig. 9, it is worthwhile to note that they have narrow spectral peaks at relatively high reduced frequencies from 0.16 to 0.6. Toy and Tahouri (1988) suggested that the three-dimensionality of the airflow around a semi-cylindrical structure is closely related to the interaction between the spanwise shear layers separated from the side surfaces of the model, and hence the vortex shedding might be formed in the wake. Thus, the reason why such a narrow peak appear for the drag force spectra is considered to be associated with the shedding frequency of the

spanwise shear layers, at which the wind pressure spectra would also show clear peaks at approximately these central frequencies.
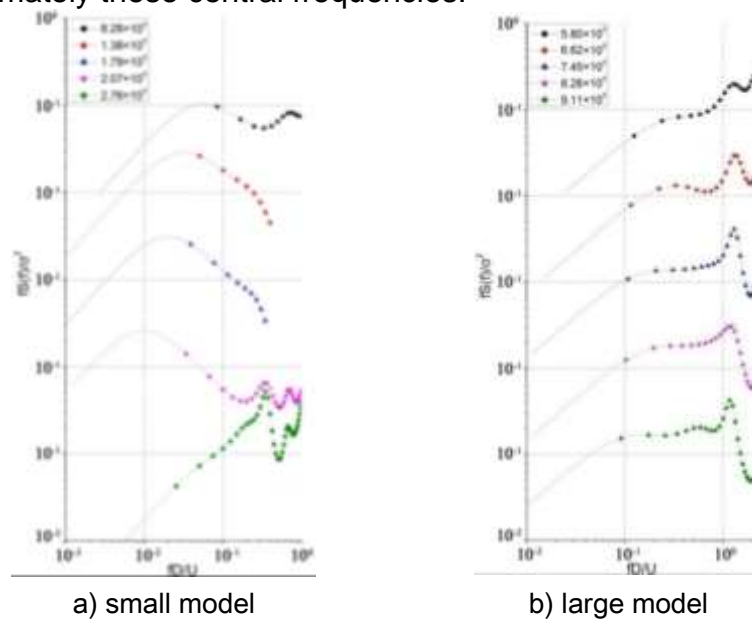

a) small model   b) large model

Fig. 8 The power spectra of the fluctuating lift forces in smooth flow

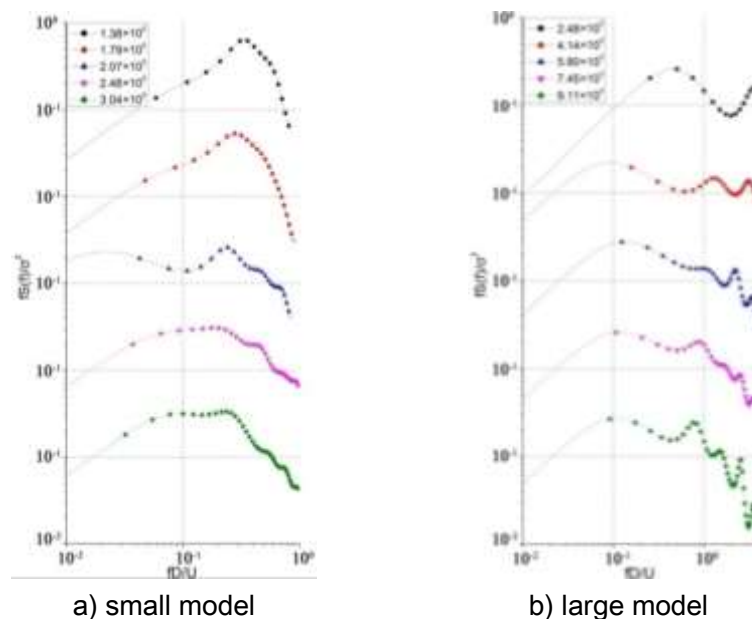a) small model   b) large model

Fig. 9 The power spectra of the fluctuating drag forces in smooth flow

4. Conclusions

This paper focuses on the experimental investigation of the effects of Reynolds number on the aerodynamic characteristics of a dome roof with rise ratio(H/D) of 0.25 in approximately uniform flows. In smooth flow, it is found the mean wind force coefficients (C_d and C_l) together with the position of the separation point are

significantly influenced by the Reynolds number in a transitional Re range of 1.66×10^5 to 2.48×10^5, and these aerodynamic coefficients become relatively stable when Re > 2.48×10^5. The characteristics of the fluctuating wind pressures and forces at various Re numbers were also clarified by the fluctuating pressure distribution and power spectra. It was observed that the Reynolds number has a significant influence on the distribution patterns of the fluctuating wind pressure and power spectra, and the peak frequency was found to shift towards higher frequency level with Re increasing.

REFERENCES

Cheng C M, Fu C L. (2010) "Characteristic of wind loads on a hemispherical dome in smooth flow and turbulent boundary layer flow", J. Wind Eng. Ind. Aerodyn., 98(6): 328-344.

Meroney R N, Letchford C W, Sarkar P P(2002), "Comparison of numerical and wind tunnel simulation of wind loads on smooth, rough and dual domes immersed in a boundary layer". Wind and Structures, 5(2/4): 347-358.

Savory E, Toy N(1986), "Hemisphere and hemisphere-cylinders in turbulent boundary layers". J.Wind Eng. Ind. Aerodyn. 1986, 23: 345-364

Toy, N., Tahouri, B.(1988), "Pressure distributions on semi-cylindrical structures of different geometrical cross-sections", J. Wind Eng. Ind. Aerodyn. 29(1), 263-272.